Journal of Applied Physics

RESEARCH ARTICLE | MARCH 13 2018

Percolative multi-susceptible PVDF/NZFO composite films with triply controlled high dielectric and magnetic properties

Wenjia Zhao; Jiaqing Gong; Hon Fai Wong; Zongrong Wang; Chi Wah Leung; Ning Ma; Piyi Du

J. Appl. Phys. 123, 104104 (2018)
https://doi.org/10.1063/1.5008791

Percolative multi-susceptible PVDF/NZFO composite films with triply controlled high dielectric and magnetic properties

Wenjia Zhao,[1] Jiaqing Gong,[1] Hon Fai Wong,[2] Zongrong Wang,[1] Chi Wah Leung,[2] Ning Ma,[1] and Piyi Du[1]
[1]*State Key Laboratory of Silicon Materials, School of Materials Science and Engineering, Zhejiang University, Hangzhou 310027, China*
[2]*Department of Applied Physics, Hong Kong Polytechnic University, Hung Hom, Hong Kong*

(Received 10 October 2017; accepted 22 February 2018; published online 13 March 2018)

Flexible multi-field susceptible films with remarkable properties and high data storage characteristics are promising in modern electronics. In this work, the percolative $Ni_{0.5}Zn_{0.5}Fe_2O_4$ (NZFO)/polyvinylidene fluoride (PVDF) composite films with both high permittivity and significant magnetic properties are prepared by dip coating on ITO/glass substrates. The highest permittivity of 74 is achieved with the NZFO volume ratio close to the percolation threshold, which is 20 times higher than that of pure PVDF. Meanwhile, the dielectric loss is kept below 0.1. The saturation and remanent magnetizations of composite films are 42.04 and 5.70 emu/g and the permeability is ~3.105, reaching 60%–80% of those in the single phase NZFO. Detailed analysis shows that the high permittivity of the composite film is triply controlled simultaneously by the intrinsic characteristic of the PVDF phase, Kirkpatrick's hybridization model and microcapacitor behavior. It will be of broad interest to control both high dielectric and magnetic properties at the same time of many other flexible and susceptible storage devices. *Published by AIP Publishing.*
https://doi.org/10.1063/1.5008791

INTRODUCTION

With the coexistence of ferroelectric and ferromagnetic properties in a single system, the multi-field susceptible composite can find numerous applications in modern electronic devices, providing both inductance and capacitance simultaneously. In recent years, there have been many kinds of ferroelectric-ferromagnetic composites, which are potential candidates for data storage,[1,2] sensors[3] and actuators,[4] among many others. The ceramic-polymer composite is one of the most important ferroelectric composites, which has typical advantages in flexibility and low dielectric loss. Polyvinylidene fluoride (PVDF) is a well-known flexible matrix with more favorable dielectric properties than other polymers, while its permittivity is still too low to meet the requirements of many electronic fields.[5–7] To address the low permittivity issue, many efforts have been spent by scientists.[8–12]

According to the percolation theory, the permittivity of the composite with conductive and dielectric phases will increase dramatically with the conductive phase toward the percolation threshold. The inner micro-capacitors seem to be formed in a series along the external field, in which the conductive phases act as electrodes and the dielectric phases are insulating media. The larger the number of micro-capacitors structured in a unit space, the higher the apparent permittivity. When the conductive phase approaches the percolation threshold, the apparent permittivity of the composite will be increased due to the significant decrease in thickness of the dielectric layer between the conductive electrodes. Thus, composites with high permittivity could be obtained based on the combination of the matrix with low intrinsic permittivity and the conductive filler, although the detailed mechanism of the increase in permittivity needs to be further revealed.[8–16]

In this work, we proposed a PVDF/nickel-zinc ferrite (NZFO) composite, in which NZFO acts as a conductive filler due to its much higher conductivity than that of the PVDF matrix, while it is applied as the ferromagnetic phase. The percolative system may be formed in the dual phased ferroelectric/ferromagnetic system, and super-high permittivity may be obtained near the threshold, solving the issue of low dielectric nature of PVDF although it has almost the largest one in flexible polymers. Moreover, in the composite film, the ferrite nanoparticles will be well-enwrapped by the dielectric polymer matrix and the general problem of relatively high dielectric loss of the percolative system will be most probably overcome. It is worth noting that PVDF is a typical flexible ferroelectric polymer with relatively high intrinsic permittivity at room temperature, and NZFO is a typical ferromagnetic phase which has higher conductivity, like many other ferrites, than the polymer. Based on the universal flexible dual phased ferroelectric/ferromagnetic system, the dielectric and magnetic properties of the composite films are investigated. The percolation mechanism of the composite is sought in detail and the triply controlled high dielectric and magnetic properties of the polymer/ferrite system is revealed, which would be of broad interest to control both high dielectric and magnetic properties at the same time of many other systems.

EXPERIMENTAL

$Ni_{0.5}Zn_{0.5}Fe_2O_4$ (NZFO) nanoparticles are synthesized by the self-combustion reaction of nitrate-citrate sol using ferric nitrate, zinc nitrate and nickel nitrate as precursor

chemicals.[17–19] Initially, the precursor chemicals are dispersed in de-ionized water separately. After that, the ionic solutions are mixed together to get a sol solution with citric acid as a complexing agent. The derived sol is made into raw powder by the self-combustion reaction in an electric oven, and then it is calcined at 750 °C for 2 h in a muffle furnace to get NZFO nanoparticles.

The NZFO nanoparticles are modified with vinyltriethoxysilane (VTES) solution as silane coupling agents, which is prepared with ethylic acid and ethanol as a mixing solvent with pH between 3 and 4.[20] The hydrolysis of VTES is completed after 1-h stirring at room temperature. After that, the NZFO particles are added to the solution for 20 min with ultrasonic dispersion. The precipitates of VTES-enwrapped NZFO powders are then dried and disaggregated from agglomeration in an agate mortar and grounded for further use as modified NZFO powders.

The polar solvent, *N*,*N*-dimethylformamide (DMF) is chosen as a solvent for PVDF powder (FR904, Shanghai 3 F New Material Co., Ltd.). Various amounts of NZFO nanoparticles with and without surface modification are dispersed in DMF and then treated ultrasonically for 30 min to form a series of homogeneous NZFO precursors. To get a composite precursor mixture, same amount of PVDF is dissolved in the obtained series of NZFO precursors at 60 °C for 120 min to keep the weight ratio of PVDF to DMF of NZFO precursors to be consistent as 1:10 for all mixtures. The precursor mixtures of composites are obtained after cooling to room temperature. The composite films of NZFO/PVDF are prepared by a dip coating method on an ITO electrode substrate at a withdrawal speed of 1 cm/min and then heat treated at a temperature of 70 °C for 24 h.

The phase formation, the microstructure and the morphology of NZFO particles and the composite films are characterized by X-ray diffraction (XRD), scanning electron microscopy (SEM) and high-resolution transmission electron microscopy (HRTEM). Chemical bonding and formation characters of PVDF phases are measured by Fourier transform infrared spectroscopy (FTIR). The dielectric and magnetic properties of the composite films are measured using an Agilent 4294 A precision impedance analyser and a magnetic property measurement system (MPMS) equipped with a superconducting quantum interference device (SQUID) magnetometer, respectively.

RESULTS AND DISCUSSION

Figure 1 reveals the SEM morphologies of PVDF/NZFO composites annealed at 70 °C with different volume ratios of NZFO modified with VTES. The dome-like morphology appears in PVDF thin films without and with different content (expressed in volume fraction throughout the article) of NZFO lower than 60%. The higher the content of NZFO in PVDF, the smaller the spherulite size. The clusters of NZFO powders appear, while the dome-like morphology almost disappears with the NZFO particle content higher than 40% in the composite. They begin to aggregate heavily with further increase in the content of NZFO to 60%. After that, the composite film cannot even be formed very well when the content of NZFO has reached 70% [Fig. 1(f)].

Figure 2 shows TEM images of the NZFO powder without and with surface modification with an average size from 60 to 100 nm. Apparently, there is a thin amorphous layer with a thickness of about 2 nm covering the NZFO particles uniformly after surface modification [Fig. 2(d)], while nothing can be seen on the surface of particles without modification [Fig. 2(c)]. The layer covering NZFO is actually the hydrolysate of VTES, which enwrapped tightly the NZFO particles through interaction between the -Si(OH) group of VTES and the hydroxyl group on the surface of NZFO. The vinyl group, which is on the other side of the VTES molecule, has good compatibility with PVDF. Thus, as a bridge layer, VTES can improve the composite film formation in which the NZFO particles are uniformly dispersed in the organic PVDF matrix. At the same time, with the VTES enclosing the NZFO [Fig. 2(d)], the PVDF molecular chains will come in contact with NZFO powders as the nucleating centre tightly through VTES and form the dome-like phase. The more the nanoscale NZFO centre is in the composite, the smaller the spherical size of PVDF, because less amount of PVDF is assigned to the high content of NZFO centres covered by VTES. Therefore, the spherical size decreases in the composite with the NZFO content from 0% to 30%, and then the spherical morphology disappears above the NZFO content of 40%. However, above 40% of NZFO, the NZFO clusters begin to appear and the amount increases with increasing content of NZFO in the composite system. Especially, in the system with high content of NZFO above 60%, as shown in Fig. 1(e), the NZFO clusters aggregated in the composite film. It is obvious that the PVDF/NZFO composite film formed with the NZFO nanoparticles is dispersed uniformly below 40%. The NZFO clusters begin to aggregate together when their content was further increased to above 40% in the composite film.

Figure 3(a) shows the XRD patterns of a single phase of NZFO nanoparticles prepared by self-combustion. It is obvious that the NZFO nanoparticle is a typical spinel phase, as shown in Fig. 3(a).[20] XRD patterns of the PVDF/NZFO composite films annealed at 70 °C with various content of NZFO powder are shown in Fig. 3(b). Both phases of NZFO and PVDF appear. Peak intensities of NZFO increase clearly with the increase in the content of NZFO. The peak intensity of the PVDF crystalline phase of both α- and β-phases typically at $2\theta = 20°$ (Refs. 21 and 22) increases firstly from 0% to 10% of NZFO and then decreases with NZFO content of 10% to 60%. According to the peak intensity of PVDF at $2\theta = 20°$, the highest content of the crystalline phase including both α-PVDF and β-PVDF seems to appear in the composite film with 10% of NZFO. In general, crystallization of PVDF on the substrate such as glass results from heterogeneous nucleation.[5,21] For the single phase PVDF, its crystallization is mainly determined by the substrate as a heterogeneous source. However, for composite films as shown in this case, the crystallization of PVDF is influenced not only by the substrate but also by the second phase NZFO, which can be act as a heterogeneous nucleus. When the NZFO particles are added into the film, it is of great

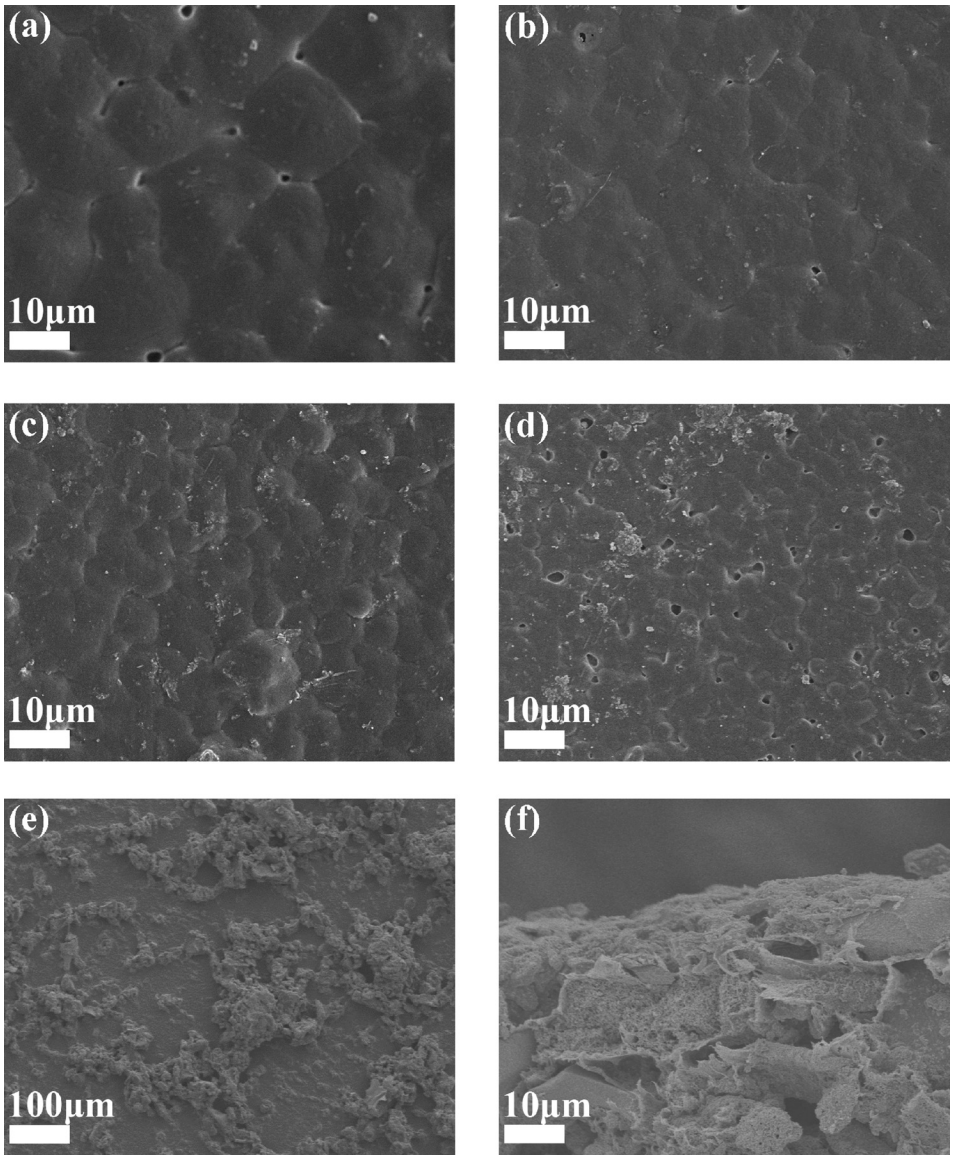

FIG. 1. SEM surface morphology of PVDF/NZFO composite films with different volume fractions of NZFO particles: (a) 0%, (b) 3%, (c) 14%, (d) 40%, and (e) 60%. (f) The cross-sectional image of the sample with 70% NZFO.

importance in controlling the formation of the PVDF crystalline phase. The crystallization is thus enhanced with increasing NZFO to 10% in the composite as shown in Fig. 3(b). However, in this work, it is revealed that the peak intensity of PVDF declined with the addition of more NZFO into the composite from 10% to 60% as shown in Fig. 3(b). There may be two important reasons for the trend. One reason is that, with increasing NZFO content, starting from 10%, the relative content of PVDF apparently decreased in the composite. Hence, the higher the content of NZFO is in the composite, the lower the fraction of PVDF and lower the peak intensity of PVDF in the composite. The other one is that the crystalline phase of PVDF may be disturbed to form by the unlike phase of NZFO due to the introduction of deficiencies into PVDF. The higher the content of NZFO in the composite, the more the deficiencies will be introduced into PVDF and the lower the crystallinity of PVDF.

As a matter of fact, both α-PVDF and β-PVDF crystalline phases will form predominantly in the composite film. Figure 4(a) shows the FT-IR spectra of NZFO/PVDF composites annealed at 70 °C with different content of NZFO from 0% to 60%. The vibration bands at 408 cm^{-1}, 532 cm^{-1}, 612 cm^{-1}, 765 cm^{-1}, 796 cm^{-1}, 855 cm^{-1}, and 976 cm^{-1} shown in spectra are attributed to the α-phase of PVDF and the bands at 511 cm^{-1} and 840 cm^{-1} correspond to the β-phase of PVDF, respectively.[21,23–25] Obviously, according to Fig. 4(a), all the composite films consisted of two phases such as α-PVDF and β-PVDF with the addition of NZFO. The relative fraction of both α- and β-phases in a sample can be calculated based on absorption peaks according to the equation as follows:[26]

$$F(\beta) = \frac{X_\beta}{X_\alpha + X_\beta} = \frac{A_\beta}{1.29A_\alpha + A_\beta}, \quad (1)$$

where X_α and X_β represent the crystallinity of α- and β-phases, respectively, and A_α and A_β represent the absorbance at 765 cm^{-1}, and 840 cm^{-1}, respectively. The fraction of β-PVDF in the NZFO/PVDF composite film is shown in Fig. 4(b). It shows that the fraction of β-PVDF in the two phases increases with the increase of volume content of NZFO in the NZFO/PVDF composite film. β-PVDF increases sharply from about 20% to above 90% with NZFO from 0 to about

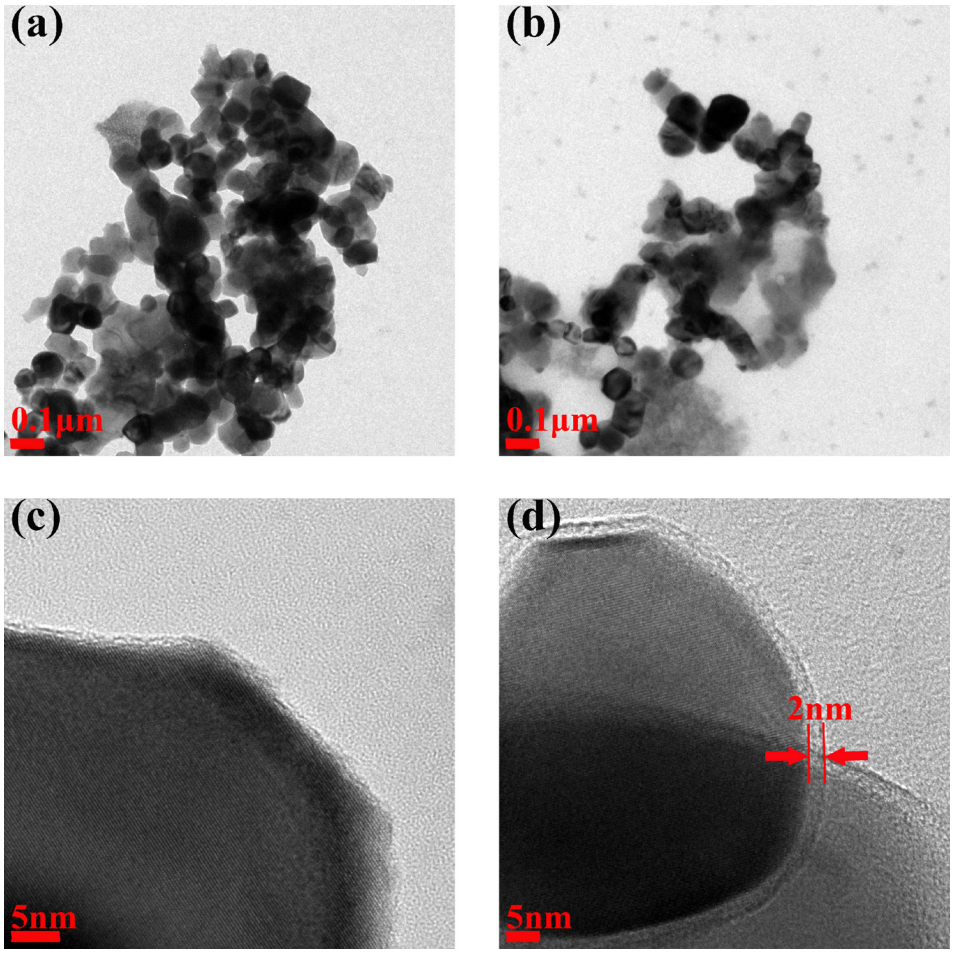

FIG. 2. TEM images of NZFO powder without (a and c) and with (b and d) surface modification by VTES.

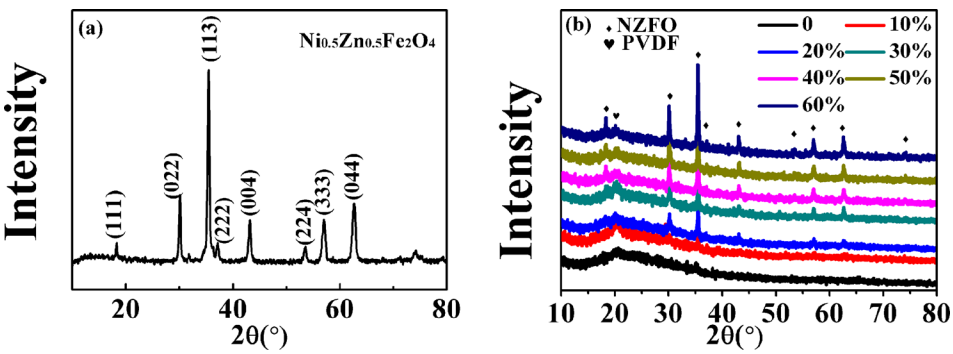

FIG. 3. XRD patterns of (a) single phased NZFO nanoparticles and (b) PVDF/NZFO composite films annealed at 70 °C with various content of NZFO.

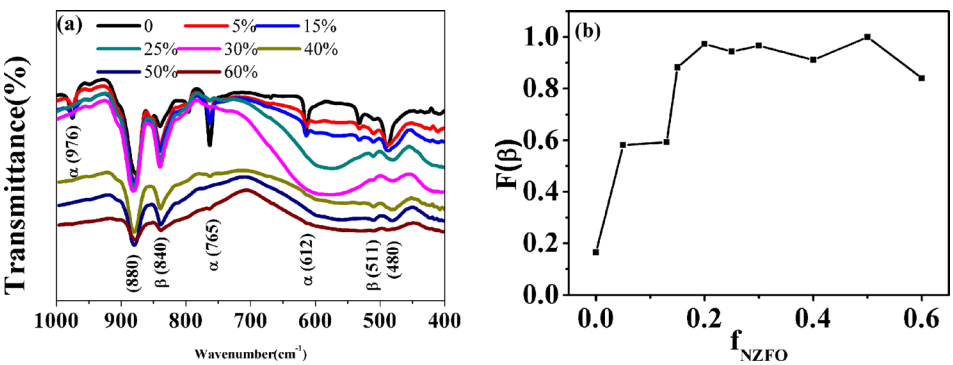

FIG. 4. (a) FTIR spectra of PVDF/NZFO composites and (b) relative content of the β phase in all membranes calculated by Eq. (1).

15 vol. %, and remains almost stable above NZFO of 15% in the composite.

It is known that as PVDF dissolved in DMF solvent, the interaction between dipoles of the C = O group in DMF and the CH_2-CF_2 group in PVDF will occur to disentangle the chains of PVDF in DMF.[27–29] In addition, as the film gets deposited on the glass substrate, the formation of β-PVDF is attributed to the interaction between the glass substrate and

PVDF molecular chains. When the PVDF solution is deposited, many hydrogen bonds will form between hydroxyl groups on the substrate and F atoms in the PVDF molecular chains, which are easily movable in the solution. The F atoms on one side of the PVDF molecular chain are thus induced easily to arrange along the substrate in the same orientation based on the existing hydrogen bonds. This ordered structure is in favour of forming β-PVDF in the film. Furthermore, in this work, when the modified NZFO particles are added to the PVDF, as has been discussed above, PVDF will enwrap the NZFO particles and bond tightly with NZFO through VTES in-between. The new contacting interfaces are introduced significantly into the composite between PVDF and NZFO. In this case, the NZFO phase has the same influence as the glass substrate on the formation of β-PVDF, and the probability of contact between PVDF and the substrate as well as NZFO increases. The crystalline phase of PVDF, mainly the β-PVDF phase instead of α-PVDF, generally forms in PVDF without NZFO.

Figure 5(a) shows the frequency dependence of permittivity of NZFO/PVDF composite films annealed at 70 °C with different content of NZFO. The Debye-like response of the dielectric constant for the whole frequency range of interest occurs in all the composite films with different NZFO content from 0% to 60%. For a specific frequency of 200 kHz, the dielectric constant of the film increases significantly from 3.6 to about 73.8, as shown in Fig. 5(b). The permittivity increases rapidly from 3.6 to about 16.0 with NZFO below 15%, and then changes very slowly to about 20 with increasing NZFO content to 40 vol. % in the composite film. After that, the permittivity of the composite film increases sharply to about 73.8 with continuously increasing NZFO content to 60%, which is about 20 times higher than that without NZFO. As discussed above for the formation of the PVDF film, the β-PVDF phase increases to ~100% in the whole crystalline phase of PVDF with the increase of NZFO content to above 15%. As is known, the β-PVDF phase contributes to permittivity predominantly due to its ferroelectric property. The permittivity thus increases from 3.6 to 16.0, as the NZFO content increased to about 15%, which is about 4 times as high as that of the PVDF film without a nucleating centre of NZFO particles, and thus with low content of the β-PVDF phase. It implies that the significant increase in permittivity is mainly attributed to the increase in β-PVDF in the composite film with NZFO below 15%.

After that, as revealed above, the permittivity increases slowly from 16 to 20 with the increase of NZFO from 15% to 40% in the composite. Actually, it is known that the electron hopping between Fe^{2+} and Fe^{3+} ions generally occurs in NZFO, and it also contributes to the permittivity of the ferrites ceramics based on the inhomogeneous conductivity.[30–34] It implies that the permittivity of the composite film will be attributed to the hybridization of both permittivities of the two constituent phases. In the concept of an effective hybrid dielectric model, the permittivity of the composite can be analysed using Kirkpatrick's compound law[35]

$$f_{NZFO}\frac{\varepsilon_{NZFO}-\varepsilon}{\varepsilon_{NZFO}+\left(\frac{1}{f_c}-1\right)\varepsilon}+(1-f_{NZFO})\frac{\varepsilon_{PVDF}-\varepsilon}{\varepsilon_{PVDF}+\left(\frac{1}{f_c}-1\right)\varepsilon}=0, \tag{2}$$

viz,

$$\varepsilon=\frac{(f_c+f_{NZFO}-1)\varepsilon_{PVDF}+(f_c-f_{NZFO})\varepsilon_{NZFO}}{2(f_c-1)}-\frac{\sqrt{[(f_c+f_{NZFO}-1)\varepsilon_{PVDF}+(f_c-f_{NZFO})\varepsilon_{NZFO}]^2-4(f_c-1)f_c\varepsilon_{NZFO}\varepsilon_{PVDF}}}{2(f_c-1)}, \tag{3}$$

where ε, ε_{NZFO}, and ε_{PVDF} are the permittivity of the composite film, the NZFO phase and the PVDF, respectively, including the α-, β-, and amorphous-phases and f_{NZFO} is the volume fraction of NZFO in composite films. In fact, the NZFO clusters are distributed separately in PVDF below the threshold and generally begin to contact at the threshold. When f_{NZFO} increases to 70% or above, the composite film is hard to form and the configuration of the PVDF matrix is

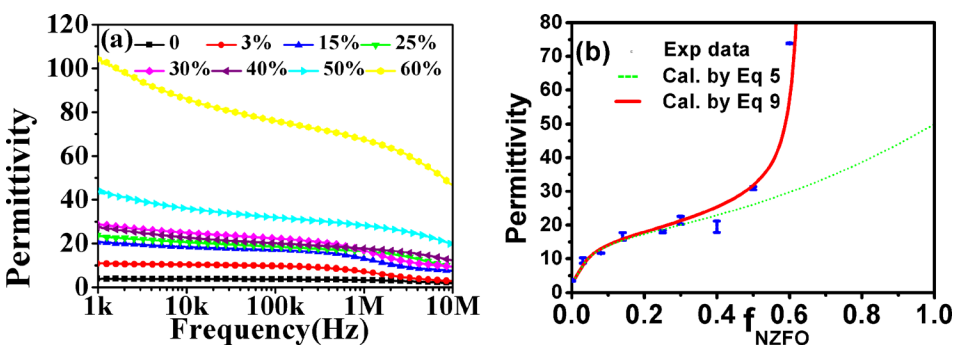

FIG. 5. Plots of permittivity of NZFO/PVDF versus (a) the applied frequency between 1 kHz and 10 MHz and (b) the NZFO fraction in the composite films at 200 kHz.

cracked completely due to excessive NZFO in the composite, as shown in Fig. 1(f). Hence, the threshold must be between $f_{NZFO} = 0.6$ and $f_{NZFO} = 0.7$.

Moreover, as is known, ε_{PVDF} used in Eq. (3) is a constant according to Kirkpatrick's model. However, as discussed above, the fraction of β-PVDF in all crystalline phases and the whole PVDF crystalline phase in the composite increases with increasing NZFO, implying that it is changeable and increases with increasing NZFO due to the increase of the β-PVDF crystalline phase in PVDF. The content of the β-PVDF crystalline phase in PVDF can be approximately considered as a function of f_{NZFO}, the volume fraction of NZFO in composite films. Hence, the ε_{PVDF} would be approximately calculated using the exponential function of f_{NZFO} as

$$\varepsilon_{PVDF} = a\exp(-c/f_{NZFO}) + b, \tag{4}$$

where a and b are coefficients related to the intrinsic characteristic of the permittivity of PVDF and c is a coefficient of β-PVDF changing with NZFO content in the composite. Inserting the changeable ε_{PVDF} into Eq. (1), Kirkpatrick's compound law can be rewritten as

$$\varepsilon_{composite} = \frac{(f_c + f_{NZFO} - 1)[a\exp(-c/f_{NZFO}) + b] + (f_c - f_{NZFO})\varepsilon_{NZFO}}{2(f_c - 1)} - \frac{\sqrt{\{(f_c + f_{NZFO} - 1)[a\exp(-c/f_{NZFO}) + b] + (f_c - f_{NZFO})\varepsilon_{NZFO}\}^2 - 4(f_c - 1)f_c\varepsilon_{NZFO}[a\exp(-c/f_{NZFO}) + b]}}{2(f_c - 1)}. \tag{5}$$

Based on this equation with the changeable ε_{PVDF} and coefficients $a = 12$, $b = 3.6$, and $c = 0.035$, $\varepsilon_{NZFO} = 40$ and $f_{NZFO} = 0.62$, the fitting curve of permittivity of the composite film versus NZFO content is shown in Fig. 5(b) as a dashed line, which agrees with experimental data well over the range of NZFO content between 0% and 40%. It implies that the permittivity of the composite film composed of NZFO and PVDF is based on Kirkpatrick's compound law, especially in the range between 15% and 40%.

However, unlike the permittivity below 40% of NZFO, it significantly deviated from that obtained from Kirkpatrick's compound law above 40% of NZFO. As has been discussed above, the electron hopping between Fe^{2+} and Fe^{3+} ions generally occurs in NZFO, and thus NZFO has relatively higher conductivity, which is 4.9×10^{-4} S/m, almost 8–9 orders higher than that of the PVDF phase of about 10^{-14} to 10^{-13}S/m. The conductor/dielectric system contributes most probably the apparently relatively high dielectric constant to the composite film due to the engineered micro-capacitors. That is, the composite will enable its dielectric constant to sharply increase with increasing conductive phase toward the percolation threshold via inducing the inner electrode as well as microcapacitors into the film.[8–12,36]

In fact, the conductive NZFO particles as the inner electrode are uniformly separated in the PVDF matrix. This makes the composite films composed of a series of microcapacitors with only a thin dielectric layer of PVDF between the electrodes of NZFO particles along the applied external field. Considering that the particle size of NZFO is d_{NZFO} and the layer thickness between NZFO particles is d_{PVDF}, when the amount of NZFO particles is large enough, the capacitance of the composite film with a thickness D and an area S is shown as below:

$$C = \frac{S}{D}\varepsilon_{PVDF}\left(1 + \frac{d_{NZFO}}{d_{PVDF}}\right) = \frac{S}{D}\varepsilon_{composite}, \tag{6}$$

where $\varepsilon_{composite} = \varepsilon_{PVDF}(1 + \frac{d_{NZFO}}{d_{PVDF}})$ is the apparent permittivity of the composite film. It is obvious that the apparent permittivity of the composite film increases significantly and nonlinearly with decreasing layer thickness of PVDF between the particle electrodes, which is controlled only by the topological dispersion of both NZFO and PVDF, thus by contributing different thicknesses of the PVDF layer with content of NZFO particles, instead of by increasing the intrinsic permittivity of PVDF. It implies that the permittivity occurs in the composite PVDF/NZFO film via designing the topological microstructure without the change in the intrinsic permittivity of the PVDF itself.

According to the percolation theory, the permittivity of the composite changing with NZFO content would also be described by the following power law:[10]

$$\varepsilon_{composite} = \varepsilon_{PVDF}\left(\frac{f_c - f_{NZFO}}{f_c}\right)^{-q}, \tag{7}$$

where q is a critical exponent. This equation actually shows a typical relationship between the dielectric constant of the composite and the content of the relatively conductive phase of NZFO. In this equation, the change in the tendency of the increment of permittivity with the fraction of NZFO based on the ε_{PVDF} in the composite is given by

$$\Delta = \varepsilon_{PVDF}\left[\left(\frac{f_c - f_{NZFO}}{f_c}\right)^{-q} - 1\right]. \tag{8}$$

Hence, in this paper, the permittivity of the composite film is the sum of Eqs. (5) and (8) with regard to β-PVDF content,

hybridization of the two constituent phases in the composite and the increment trend related to the percolation phenomenon, as shown in the following equation:

$$\varepsilon_{composite} = \left[\left(\frac{f_c - f_{NZFO}}{f_c}\right)^{-q} - 1\right][a\exp(-c/f_{NZFO}) + b] + \frac{(f_c + f_{NZFO} - 1)[a\exp(-c/f_{NZFO}) + b] + (f_c - f_{NZFO})\varepsilon_{NZFO}}{2(f_c - 1)} - \frac{\sqrt{\{(f_c + f_{NZFO} - 1)[a\exp(-c/f_{NZFO}) + b] + (f_c - f_{NZFO})\varepsilon_{NZFO}\}^2 - 4(f_c - 1)f_c\varepsilon_{NZFO}[a\exp(-c/f_{NZFO}) + b]}}{2(f_c - 1)}. \quad (9)$$

After fitting with the coefficient of q = 0.3, the permittivity calculated by this equation increases from 20 at composition around 40% of NZFO to 74 sharply near approaching 60% as shown in the solid line in Fig. 5(b), which is in good agreement with the experimental data on the PVDF/NZFO composite films over the range between 40% and 60% of NZFO. Therefore, the permittivity that increased sharply around the composition of 60% of NZFO can be attributed to the artificially structured microcapacitors inside of the conductor/dielectric system, in which the threshold fc is ∼0.62 in the NZFO volume fraction and q is 0.3.

Other than the calculated permittivity of the composite with NZFO fractions of 40% and 60% consistent with experimental data, it also agrees well with experimental data for composite with NZFO fractions between 0% and 40%. In fact, there are three typical influences on the permittivity of the composite film. The first is β-PVDF content in the PVDF matrix. It mainly controls the permittivity of the matrix of the composite film due to the formation of the β-PVDF crystalline phase in the PVDF phase with the addition of NZFO. The second is the control of compound law on permittivity based on Kirkpatrick's model due to the mixing of two phases of PVDF and NZFO. It contributes predominantly to the permittivity of the composite with medium content of NZFO without any connection among themselves. The third is the microcapacitors appearing geometrically engineered in the conductor/dielectric system. It contributes to high apparent permittivity of the composite in which the NZFO fraction is near the threshold at which large amounts of microcapacitors are formed.

Consequently, the higher the β-PVDF phase in the composite, the higher the permittivity of the composite. As the content of β-PVDF remains stable in the composite within the medium content of NZFO, the permittivity of the composite film is controlled mainly by the compound law of Kirkpatrick's and it increases slowly with increasing content of NZFO due to a little higher permittivity of NZFO than PVDF. However, the permittivity is significantly controlled by the artificial structure as the content of NZFO approaches the threshold. The closer toward the threshold, the higher the permittivity is obtained.

In this case, it increases by 3.6 times in the film with only β-PVDF compared to that with α-PVDF and β-PVDF that coexist, by another 1 time in the film with increasing content of NZFO over its medium content range based on hybridization of the two constituent phases of NZFO and β-PVDF, and by another 6 times with the contribution of the artificially engineered structure near the threshold. Therefore, the permittivity of the composite increases totally by about 20 times with increasing NZFO content to about 60% in the composite film. And it is 7 times as large as that of pure β-PVDF generally reported.[10,37]

As a consequence, the conductive NZFO nanoparticles as nucleating centres promote the formation of the β-PVDF phase with higher permittivity than that of the single PVDF phase and result in high permittivity composite films by the hybridization model. Moreover, NZFO particles also introduce the inner electrodes to form a series of microcapacitors and increase the permittivity of the composite film dramatically. The permittivity of the composite film is triply controlled simultaneously by intrinsic characteristic of the PVDF phase, Kirkpatrick's hybridization model and microcapacitor behaviour. In this way, the permittivity gets improved significantly by 20 times compared to that of PVDF film without NZFO. The superhigh permittivity appears typically near the threshold in the composite film, which is mainly contributed by the artificially engineered structure with an ultra-thin PVDF layer between conductive NZFO.

Figure 6(a) shows the frequency dependence of dielectric loss of the NZFO/PVDF composite films and Fig. 6(b) shows the minimum dielectric loss of the films with different content of NZFO. It is seen that the dielectric loss within the frequencies between several kHz and several hundreds of kHz is lower than 0.1 for all the composite film with NZFO content below 60% in volume fraction. The smallest loss is around 0.07. When the content of the magnetic filler of NZFO is between 30% and 60% with which the permittivity of the composite is quite high as 74, the dielectric loss remains below 0.1, and most of them are frequency-independent within some hundreds of kilohertz range. It implies that, not only the high permittivity, but also the low dielectric loss appearing in the PVDF/NZFO composite film with high content of magnetic NZFO, due to NZFO effectively enwrapped by PVDF although the PVDF layer is extremely thin near the threshold.

Figure 7(a) shows the magnetization of NZFO/PVDF composite films with different content of NZFO annealed at 70 °C as a function of magnetic fields between −4 and 4 kOe. The inset shows the zoomed-in curves under a magnetic field between −200 and 200 Oe. The saturation magnetization, the remanent magnetization and the coercivity of the PVDF/NZFO composite films are shown in Table I. It is

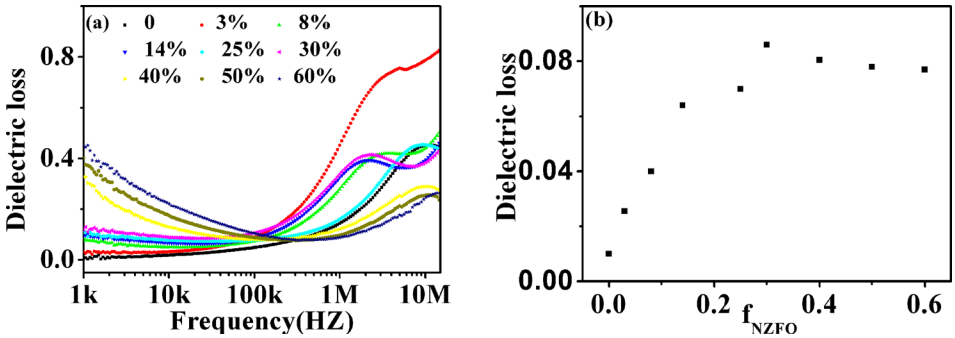

FIG. 6. (a) Plots of frequency dependence of dielectric loss of NZFO/PVDF composites with various NZFO fractions and (b) plots of the lowest dielectric loss as a function of volume fraction of NZFO in the composite films.

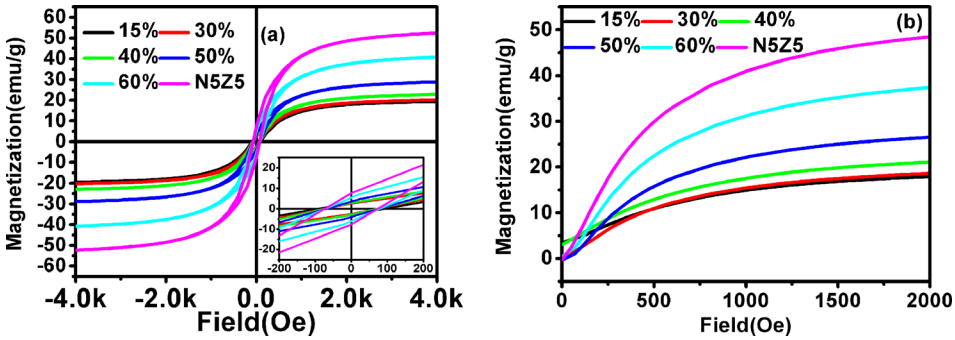

FIG. 7. (a) Magnetic hysteresis loops of NZFO/PVDF composites annealed at 70 °C with different fractions of NZFO (inset shows the enlargement curves under the magnetic field between −200 and 200 Oe) and (b) initial magnetization curves of the composite with different NZFO content as a function of the magnetic field from 0 to 2000 Oe.

seen that the typical hysteresis loops are exhibited in all the composites with different content of NZFO from 15 vol. % to 100 vol. % (i.e., pure NZFO). The saturation and remanent magnetizations of the composite films are lower than those of pure NZFO as the magnetic NZFO is surrounded by a non-magnetic polymer in the composite films.[38–40] The saturation magnetization increased from 20.29 to 42.04 emu/g and the remanent magnetization increased from 2.78 to 5.70 emu/g, respectively, upon increasing the ferrite from 15 vol. % to 60 vol. % due to the decrease of surrounding PVDF. The magnetization of the composite with 60 vol. % NZFO is kept at about 87% of 48.28 emu/g and 77% of 7.38 emu/g of pure NZFO, respectively. Figure 7(b) shows that the initial magnetization curves of the composite films changed with the external field, and the initial permeability of the composite calculated by these curves is also shown in Table I. Obviously, the more the NZFO content is, the higher the magnetisability as well as the permeability in the composite film. The permeability increases from 1.435 to 3.105 with the increase NZFO from 15 vol. % to 60 vol. %. The permeability of the composite film with 60% NZFO is maintained still at 63% of 4.964 of pure NZFO.

It is apparent that the composite with 60 vol. % of NZFO contributed simultaneously to the high dielectric properties and acceptable magnetic properties. Triply controlled permittivity reaches 74, while the dielectric loss is maintained only at 0.1. Meanwhile, the saturation and remanent magnetizations are 42.04 and 5.70 emu/g, with the initial permeability of 3.105. Obviously, the PVDF/NZFO composite film shows both high dielectric and good magnetic properties. It could be exploited in flexible electronics with multi-field susceptible properties.

TABLE I. Saturation magnetization, remanent magnetization, coercivity, and initial permeability of the PVDF/NZFO composite films with different fractions of NZFO.

Composite with NZFO (vol. %)	15%	30%	40%	50%	60%	100%
Ms(emu/g)	20.29	23.52	22.25	30.32	42.04	48.28
Mr(emu/g)	2.78	2.95	2.74	3.90	5.70	7.38
Coercivity (Oe)	95.13	72.14	71.09	73.18	75.82	73.19
Initial permeability	1.435	1.923	1.677	2.285	3.105	4.964

CONCLUSIONS

The PVDF/NZFO composite films with both high permittivity and acceptable magnetic properties are prepared by a soft chemical dip-coating method, in which the NZFO nanoparticles are dispersed uniformly in the matrix composed of single crystalline phase β-PVDF and amorphous phase PVDF. F atoms in the one side of PVDF molecular chain arrange easily in the same orientation through hydrogen bonds along NZFO, inducing β-PVDF to be formed completely as the crystalline phase in the composite film. The permittivity is controlled by the relatively high content of β-PVDF, the compound law of Kirkpatrick's model and the series of microcapacitors engineered inside appear in the PVDF/NZFO composite film. It reaches about 74 at the threshold, which is 20 times higher than that of the film with only pure PVDF. Enwrapped completely and typically by the high resistance phase PVDF, the conductive NZFO hardly contributes to the leakage current, making the dielectric loss of the PVDF/NZFO composite film still attractively low below 0.1 near the percolation threshold. Contributed by the thinner layer of PVDF between NZFOs near the threshold, the magnetic properties of the composite which has superhigh permittivity are kept well acceptable, as the saturation and remanent magnetizations are 42.04 and 5.70 emu/g and the permeability is 3.105, reaching 60%–80% of those in the single phased NZFO. It is obvious that based on the triple control on the increase in permittivity, PVDF/NZFO as well as many other composite films with both high dielectric and excellent

magnetic properties may attract us to use it as a flexible film with multi-susceptible properties as well as high performance.

ACKNOWLEDGMENTS

This work was supported by the Natural Science Foundation of China (Grant Nos. 51772269 and 51272230), Zhejiang Provincial Natural Science Foundation (Grant Nos. LY17E020006 and LF17F040003) and HKSAR (PolyU 153015/14P), respectively.

[1]J. F. Scott, Nat. Mater. **6**, 256 (2007).
[2]M. Fiebig, T. Lottermoser, D. Fröhlich, A. V. Goltsev, and R. V. Pisarev, Nature **419**, 818 (2002).
[3]J. Ma, J. Hu, Z. Li, and C. W. Nan, Adv. Mater. **23**, 1062 (2011).
[4]M. A. Zurbuchen, T. Wu, S. Saha, J. Mitchell, and S. K. Streiffer, Appl. Phys. Lett. **87**, 232908 (2005).
[5]B. H. Fan, J. W. Zha, D. Wang, J. Zhao, and Z. M. Dang, Appl. Phys. Lett. **100**, 012903 (2012).
[6]F. He, S. Lau, H. L. Chan, and J. Fan, Adv. Mater. **21**, 710 (2009).
[7]Z. M. Dang, J. K. Yuan, J. W. Zha, T. Zhou, S. T. Li, and G. H. Hu, Prog. Mater. Sci. **57**, 660 (2012).
[8]M. Wang, J. Zhu, W. Zhu, B. Zhu, J. Liu, X. Zhu, Y. Pu, P. Sun, Z. Zeng, and X. Li, Angew. Chem. Int. Ed. **51**, 9123 (2012).
[9]W. Wu, X. Huang, S. Li, P. Jiang, and T. Toshikatsu, J. Phys. Chem. C **116**, 24887 (2012).
[10]Q. Chen, P. Y. Du, L. Jin, W. J. Weng, and G. R. Han, Appl. Phys. Lett. **91**, 022912 (2007).
[11]K. Vasundhara, B. P. Mandal, and A. K. Tyagi, RSC Adv. **5**, 8591 (2015).
[12]Z. M. Dang, J. K. Yuan, S. H. Yao, and R. J. Liao, Adv. Mater. **25**, 6334 (2013).
[13]Z. H. Chen, J. Q. Huang, Q. Chen, C. L. Song, G. R. Han, W. J. Weng, and P. Y. Du, Scr. Mater. **57**, 921 (2007).
[14]A. Ameli, M. Arjmand, P. Pötschke, B. Krause, and U. Sundararaj, Carbon **106**, 260 (2016).
[15]H. Zheng, Y. L. Dong, X. Wang, W. J. Weng, G. R. Han, N. Ma, and P. Y. Du, Angew. Chem. Int. Ed. **48**, 8927 (2009).
[16]Z. R. Wang, T. Hu, L. Tang, N. Ma, C. Song, G. Han, W. Weng, and P. Du, Appl. Phys. Lett. **93**, 222901 (2008).
[17]J. Q. Huang, P. Y. Du, L. X. Hong, Y. L. Dong, and M. C. Hong, Adv. Mater. **19**, 437 (2007).
[18]Z. X. Yue, J. Zhou, L. Li, H. Zhang, and Z. Gui, J. Magn. Magn. Mater. **208**, 55 (2000).
[19]S. H. Xiao, W. F. Jiang, L. Y. Li, and X. J. Li, Mater. Chem. Phys. **106**, 82 (2007).
[20]Z. X. Yue, W. Guo, J. Zhou, Z. Gui, and L. Li, J. Magn. Magn. Mater. **270**, 216 (2004).
[21]J. Feng, L. X. Yang, W. G. Zhang, T. Gu, and W. W. Lin, Surf. Technol. **38**, 62 (2009).
[22]R. Gregorio, J. Appl. Polym. Sci. **100**, 3272 (2006).
[23]D. R. Dillon, K. K. Tenneti, C. Y. Li, F. K. Ko, I. Sics, and B. S. Hsiao, Polymer **47**, 1678 (2006).
[24]J. J. Yang, P. J. Pan, L. Hua, X. Feng, J. J. Yue, Y. H. Ge, and I. Yoshio, J. Phys. Chem. B **116**, 1265 (2012).
[25]B. S. Ince-Gunduz, R. Alpern, D. Amare, J. Crawford, B. Dolan, S. Jones, R. Kobylarz, M. Reveley, and P. Cebe, Polymer **51**, 1485 (2010).
[26]Y. L. Liu, Y. Li, J. T. Xu, and Z. Q. Fan, ACS Appl. Mater. Interfaces **2**, 1759 (2010).
[27]A. Salimi and A. A. Yousefi, Polym. Test. **22**, 699 (2003).
[28]R. Gregorio and E. M. Ueno, J. Mater. Sci. **34**, 4489 (1999).
[29]W. Z. Ma, J. Zhang, and X. L. Wang, J. Mater. Sci. **43**, 398 (2008).
[30]Y. P. Guo, Y. Liu, J. L. Wang, R. L. Withers, and H. Chen, J. Phys. Chem. C **114**, 13861 (2010).
[31]X. J. Zhao, J. Cheng, J. Zhang, S. J. Chen, and X. L. Wang, J. Mater. Sci. **47**, 3720 (2012).
[32]K. Iwauchi, Jpn. J. Appl. Phys., Part 1 **10**, 1520 (1971).
[33]A. M. Abdeen, J. Magn. Magn. Mater. **192**, 121 (1999).
[34]A. R. Lamani, H. S. Jayanna, P. Parameswara, R. Somashekar, Ramachander, R. Rao, and G. D. Prasanna, J. Alloys Compd. **509**, 5692 (2011).
[35]I. H. Gul, W. Ahmed, and A. Maqsood, J. Magn. Magn. Mater. **320**, 270 (2008).
[36]H. Zheng, L. Li, Z. J. Xu, W. J. Weng, G. R. Han, N. Ma, and P. Y. Du, J. Appl. Phys. **113**, 044101 (2013).
[37]Y. Deng, Y. J. Zhang, and Y. Z. Song, Rare Met. Mater. Eng. **38**, 583 (2009).
[38]Y. Song, Y. Shen, H. Liu, Y. Lin, M. Li, and C. W. Nan, J. Mater. Chem. **22**, 16491 (2012).
[39]A. S. Bhatt, D. K. Bhat, and M. S. Santosh, J. Appl. Polym. Sci. **119**, 968 (2011).
[40]B. Xiao, N. Ma, and P. Y. Du, J. Mater. Chem. C **1**, 6325 (2013).